

The response of the algae *Fucus virsoides* (Fucales, Ochrophyta) to Roundup® solution exposure: A metabolomics approach[☆]

S. Felline ^{a,1}, L. Del Coco ^{b,1}, S. Kaleb ^c, G. Guarnieri ^{a,b}, S. Frascchetti ^{d,e}, A. Terlizzi ^{c,e},
F.P. Fanizzi ^{b,*}, A. Falace ^c

^a CoNISMa, Piazzale Flaminio 9, 00196, Roma, Italy

^b Department of Biology, Environmental Sciences and Technologies, University of Salento, 73100, Lecce, Italy

^c Department of Life Sciences, University of Trieste, 34127, Trieste, Italy

^d Department of Biology, University of Naples Federico II, 80926, Napoli, Italy

^e Stazione Zoologica Anton Dohrn, 80121, Napoli, Italy

ARTICLE INFO

Accepted 27 July 2019

Keywords:

Glyphosate-based herbicide

Macroalgae

Coastal pollution

Metabolomics

Fucus virsoides

ABSTRACT

Glyphosate, as a broad-spectrum herbicide, is frequently detected in water and several studies have investigated its effects on several freshwater aquatic organisms. Yet, only few investigations have been performed on marine macroalgae. Here, we studied both the metabolomics responses and the effect on primary production in the endemic brown algae *Fucus virsoides* exposed to different concentration (0, 0.5, 1.5 and 2.5 mg L⁻¹) of a commercial glyphosate-based herbicide, namely Roundup®. Our results show that Roundup® significantly reduced quantum yield of photosynthesis (F_v/F_m) and caused alteration in the metabolomic profiles of exposed thalli compared to controls. Together with the decrease in the aromatic amino acids (phenylalanine and tyrosine), an increase in shikimate content was detected. The branched-amino acids differently varied according to levels of herbicide exposure, as well as observed for the content of choline, formate, glucose, malonate and fumarate. Our results suggest that marine primary producers could be largely affected by the agricultural land use, this asking for further studies addressing the ecosystem-level effects of glyphosate-based herbicides in coastal waters.

1. Introduction

The continuous and accelerating degradation and loss of marine ecosystems is a prominent concern worldwide (Lotze et al., 2006; Halpern et al., 2015), able to compromise the delivery of important goods and services to human society (Barbier, 2011). The management of these issues is very challenging for coastal ecosystems because they are particularly exposed to multiple threats acting both in the ocean and on land. Regarding land-based threats, it has been demonstrated that the conversion of native terrestrial vegetation for agriculture, urbanization and industry purposes is conducive on an increase of runoff, which in turn can lead to degradation and die-offs of coastal ecosystems such as coral reefs

(Fabricius, 2005), seagrass meadows (Waycott et al., 2009) and macroalgal beds (Airoldi & Beck, 2007). As a consequence, the conservation of coastal species, habitats and ecosystems, urgently needs an increase of knowledge of land-sea interactions in order to identify major drivers of change and set cross border management strategies across different ecosystem compartments (Beger et al., 2010).

Recently, attention has been raised about possible threats to coastal systems resulting from the use of herbicides on land (e.g. Nödler et al., 2013). The widespread employ of herbicides for decades resulted in their ubiquitous presence in the environment, and the ensuing contamination of water systems through spray drift, leaching, surface runoff during rainfall events (Botta et al., 2009; Salem et al., 2016). Glyphosate (N-[phosphonomethyl] glycine) has become one of the most popular non-selective systemic herbicide applied in the world, because of its acknowledged unique properties (low mammalian toxicity, high efficacy due to a unique systemic action *via* basipetal and acropetal translocation and relatively low price (Annett et al., 2014; Komives & Schröder, 2016). The

[☆] This paper has been recommended for acceptance by Sarah Harmon.

* Corresponding author. Dipartimento di Scienze e Tecnologie Biologiche ed Ambientali Centro Ecotekne Pal. B - S.P. 6, Monteroni, Lecce, Italy.

E-mail address: fp.fanizzi@unisalento.it (F.P. Fanizzi).

¹ These authors contributed equally to this work.

chemical was synthesized in 1950 and patented ten years later not as herbicide but as a chelator (Komives & Schröder, 2016). The herbicidal effects were discovered at Monsanto Chemical Company and the production of the first glyphosate-based commercial herbicide (Roundup®) began in 1974. Dilution and several factors (i.e., pH, water alkalinity, trophic state) affect glyphosate fate and its actual concentrations in aquatic environments. Yet, its huge applications and relatively long half-life (7–315 days) make it one of the most widespread emergent pollutant (Mercurio et al., 2014; Wang et al., 2016). Glyphosate has been listed in the 25 storm water priority pollutants (Eriksson et al., 2007) and it has been detected in streams, lakes, estuaries and other aquatic ecosystems (Widenfalk et al., 2008; Komives & Schröder, 2016; Salem et al., 2016). In plants, its primary herbicidal effect is due to the inhibition of an enzyme of the shikimate pathway (5-enolpyruvylshikimate-3-phosphate synthase) which, in turn, inhibits the aromatic amino acids synthesis (i.e., L-phenylalanine, L-tyrosine, and L-tryptophan) (Komives & Schröder, 2016; Wang et al., 2016). As result, the glyphosate leads to a halt of proteins and secondary compounds (i.e., auxins and polyphenols) synthesis (Sáenz et al., 1997). Additional side effects of glyphosate on plant physiology are damage to chloroplasts, membranes and cell walls, reduction of photosynthesis, respiration, chlorophyll and nucleic acid synthesis (Hernando et al., 1989; Schaffer & Sebetich, 2004). The toxicity of glyphosate-based herbicide (GBH) formulations has been investigated on several aquatic organisms (i.e. Mitchell et al., 1987; Kreutzweiser et al., 1989; Relyea, 2005; Stachowski-Haberkorn et al., 2008; Vendrell et al., 2009; Arunakumara et al., 2013), showing that effects mainly rely on dose and formulation tested. Yet, only few investigations have been performed on macroalgae (BurrIDGE & Gorski, 1998; Pang et al., 2012; Kittle & McDermid, 2016; Falace et al., 2018).

In temperate seas, such as the Mediterranean Sea, macroalgal beds dominated by Fucales have a crucial role in supporting the biodiversity and functioning of coastal rocky shores (Thibaut et al., 2005). These habitats are becoming rare at basin scale at an alarming rate. Urbanization, sedimentation and general pollution have been advocated as the main drivers of their loss or degradation (Airoldi & Beck, 2007). More recently the study carried out by Falace et al. (2018) on *Fucus virsoides* (Fucales, Ochrophyta) highlighted detrimental effect on the brown algae even if exposed at relative low GBH concentrations and for short time. The toxic effects highlighted by the study in laboratory conditions are irreversible leading to the seaweed's death. *F. virsoides* is a threatened macroalgal species endemic of the Adriatic Sea (Orlando-Bonaca et al., 2013) and it is included in the Red List of Threatened Species (IUCN, 2016). As it commonly characterizes the intertidal fringe, there is a general consensus that, as well as other species occurring in the same habitat, it can be severely threatened by pesticides and fertilizers coming from agricultural activities. Investigations concerning the ability of this species to cope with the impacts of agriculture practices are, therefore, urgently needed (Falace et al., 2018).

To date the metabolic pathways affected by this herbicide are still unknown. In this study, we made an attempt in this direction investigating, for the first time, the effects of different concentration of glyphosate-commercial formulation (Roundup®) on *F. virsoides* by a metabolomic approach. In the last decade, metabolomics showed considerable potential as a tool for monitoring the response of biota to pollutants (Wu & Wang, 2011; Zhang et al., 2011; Wu et al., 2011, 2012; Zou et al., 2014). Nuclear magnetic resonance (NMR) technique has been widely used in metabolomics and metabolite profiling (Liu et al., 2011; Farag et al., 2012; Zou et al., 2014). NMR based analyses make possible the unravelling

of complex mixtures providing the simultaneous identification of endogenous compounds and xenobiotics without coupling to a separation technique (Sobolev et al., 2005; Barding et al., 2012; Dunn et al., 2013; Girelli et al., 2018). NMR spectroscopy has been used in macroalgae metabolomics mainly for the characterization of species (Gupta et al., 2013; Belghit et al., 2017; Palanisamy et al., 2018) and ecotypes (Greff et al., 2017a) but also to understand the metabolic transitions in response to environmental changes (Gaubert et al., 2019) or biological interactions (Nylund et al., 2011; Greff et al., 2017b). Recently, NMR based-metabolomics was applied to investigate the effects of Cu pollution on an algal species (Zou et al., 2014). This study represents the first attempt to characterize the metabolome profile of the brown algae *F. virsoides* under GBH (i.e. Roundup®) stress, using ¹H and ³¹P NMR spectroscopy.

2. Materials and methods

2.1. Laboratory experimental setting

Healthy apical fronds of *Fucus virsoides* were collected in December 2017 during the low tide in the Gulf of Trieste-Northern Adriatic (45° 46' 25.67" N, 13° 31' 52.31" E), and transported to the laboratory (within 1 h) in insulated containers under dark conditions and low temperature. All samples were promptly cleaned with a brush and rinsed with filtered ambient seawater (0.22 mm filters membrane), to remove epibionts and sediment. A random subset of nine apical fronds were freeze-dried in order to have a metabolomic baseline information for the *in situ* conditions (test set). Instead, as far as the stress trial, the remaining samples were acclimatized for 24 h to laboratory conditions. In particular, temperature (12 °C) and photoperiod (9 L: 15 D) were selected to reflect sampling site reference conditions. Light irradiance, provided by LED lamps (AM366 Sicce USA Inc., Knoxville, USA), was set at 70 μmol photons m⁻²s⁻¹ and measured with a LI-COR LI-190/R Photometer (LICOR-Biosciences, Lincoln, NE, USA). The experiment tested the potential modification of *F. virsoides* metabolic profiles after a short exposure (24 h) to the commercial isopropylamine salt formulation of glyphosate (Roundup® Power 2.0, Monsanto Europe S.A.). Specifically, four concentrations of the GBH were used, namely 0 (Controls: C), 0.5 (G05), 1.5 (G15) and 2.5 (G25) mg L⁻¹. The commercial formulation Roundup® Power 2.0 (Monsanto Europe S.A.) was mixed in a volumetric flask with the filtered seawater collected at the sampling site to obtain the desired concentrations. The concentrations of the glyphosate isopropylamine salt in the solution were 0, 176.5, 529.5 and 882.5 μg L⁻¹ respectively (i.e. 35.3% of the Roundup® formulation). The remaining was surfactant (i.e. 6% of the formulation) and water. Each condition was replicated in three aquaria (5 L), each containing 20 apical fronds. The position of the aquaria in the temperature and light regulated room was randomized. Constant aeration in the aquaria was provided using air pumps to keep conditions homogeneous.

After 24 h of exposure to Roundup®, 3 randomly chosen apical fronds were sampled and freeze-dried for metabolomic analysis in each of the three aquaria according to the experimental conditions (9 fronds each condition). Moreover, stress effects on *F. virsoides* were estimated by measuring the chlorophyll-fluorescence of photosystem II with a Handy PEA chlorophyll fluorimeter (Hansatech Instruments Ltd, Norfolk, UK) (Supplementary Information, Section S1).

2.2. Sample preparation and NMR measurements

Samples were prepared according to the experimental

procedure previously reported in literature (Ward et al., 2003; Girelli et al., 2017) (Supplementary Information, Section S2), and 1D and 2D NMR experiments were performed on a Bruker Avance III 600 Ascend NMR spectrometer (Bruker, Ettlingen, Germany), operating at 600.13 MHz for ^1H observation, equipped with a TCI cryoprobe (Supplementary Information, Section S3). The ^1H NMR spectra were processed using Topspin 3.5 and Amix (Analysis of Mixtures) softwares 3.9.13 (Bruker, Biospin, Italy), both for simultaneous visual inspection and the bucketing process. A simple rectangular (0.04 ppm width) bucketing procedure was applied on the entire NMR spectra and the resulting data matrix was submitted to multivariate statistical analysis to examine the intrinsic variation in the data and for classification purposes (Supplementary Information, Section S4). Moreover, the relative intensity variation in glyphosate content and among the discriminating metabolites in the groups of samples were obtained by the integration of specific signals, identified by the NMR-based untargeted multivariate analysis (Supplementary Information, Section S5).

3. Results

3.1. NMR analysis of the aqueous extract of *F. virsoides* thalli

A complex pattern of signals ascribable to polyols, polysaccharides (Bilan et al., 2002, 2014; Jégou et al., 2015; Catarino et al., 2018) and the GBH (Cartigny et al., 2004, 2008) (with the exception of controls) dominated the ^1H NMR spectra (Fig. 1). Among polyols, mannitol appeared the most abundant, with signals in the range 3.9–3.6 ppm (Jégou et al., 2015). The presence of the seaweed polysaccharides complex was mainly identified as fucoidan, phlorotannins, fucoxanthin and others (Birkemeyer et al.,

2018; Catarino et al., 2018). Among these, sulphated and acetylated sugar residues (Catarino et al., 2018) as the α -L-fucose was identified by the doublet at 5.16 ppm, its acetyl group observed as an intense signal at 2.14 ppm (^{13}C 23.2 ppm), partially overlapped with signals belonging to other metabolites (in particular methionine and glutamine) and a singlet at 1.22 ppm. Doublets at 5.22 and 4.64 ppm were assigned to alpha and beta-glucose, respectively. Other polysaccharides related NMR signals were found at low frequencies (1.09 and 0.94 ppm) (Hmelkov et al., 2018). These molecules are particularly abundant in brown algae and usually represent the main components of cell wall, as complex sulphated and acetylated forms (Li et al., 2008; Gügi et al., 2015; Catarino et al., 2018; Hmelkov et al., 2018). Moreover, they have important structural functions, being also a great source of biomolecules (Rizzo et al., 2017; Hmelkov et al., 2018). The presence of GBH was confirmed by the NMR signals at 3.10 ppm ($\text{CH}_2\text{-P}$ doublet, with a coupling constant between proton and phosphorous of 11.85 Hz) and 3.72 ppm singlet, while the isopropylammonium CH_3 groups appeared at 1.16 ppm (broad signals) and 1.30 ppm (doublet) ppm (Cartigny et al., 2004, 2008). By the analysis of the ^{31}P NMR spectra of the aqueous extracts of algal thalli, the signal related to inorganic phosphate was also observed at ~ 0.3 ppm, and an additional peak was detected at 7.72 ppm as a singlet and assigned to the glyphosate phosphorus nucleus (Cartigny et al., 2004) (Supplementary Information, Fig. S1). Other metabolites were also identified in the ^1H NMR spectra, including free amino acids (alanine, valine, leucine, isoleucine, cystine, glutamate, glutamine, methylhistidine, phenylalanine, threonine, tyrosine), organic acids (citrate, malonate, maleate, lactate, formate, fumarate) and other molecules (choline, dimethylsulfone, ATP) (Table 1).

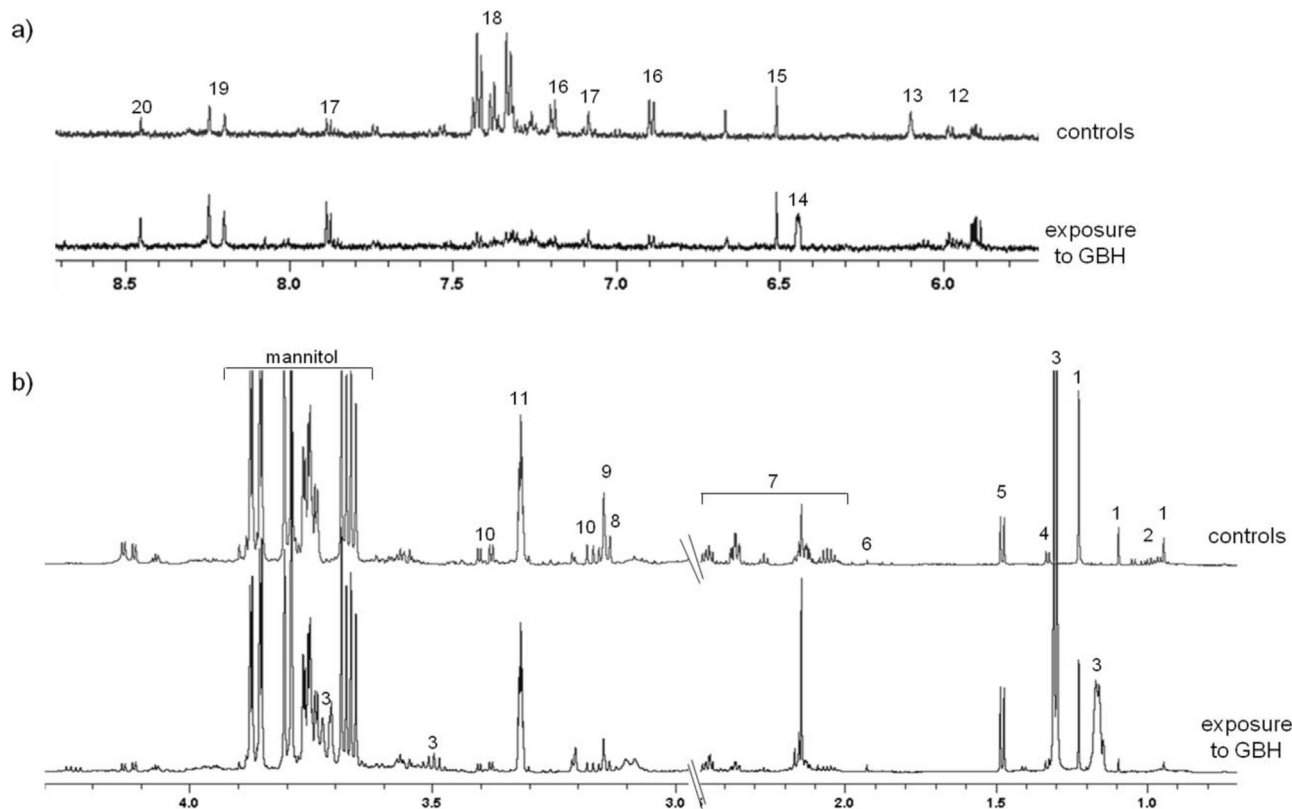


Fig. 1. ^1H NMR spectra and relative expansions of the (a) aromatic and (b) aliphatic regions of *F. virsoides* thalli aqueous extracts for controls and contaminated thalli after a short exposure to GBH. (1: polysaccharides; 2: isoleucine, leucine, valine; 3: GBH signals; 4: lactate/threonine; 5: alanine; 6: acetate; 7: methionine, glutamate/glutamine; 8: DMSO₂; 9: malonate; 10: cystine; 11: MeOH; 12: UDP-X; 13: maleate; 14: shikimate; 15: fumarate; 16: tyrosine; 17: 1-methylhistidine; 18: phenylalanine; 19: ATP; 20: formate).

Table 1

Chemical shift (ppm) and assignment of metabolite resonances (^1H and ^{13}C) identified in the 600 MHz ^1H spectrum of the aqueous extracts of *F. virsoides* thalli (Letters in parentheses indicate the peak multiplicities; s, singlet; d, doublet, t, triplet; q, quartet; m, multiplet; bs, broad signals). ^aDMSO₂: dimethylsulfone; ^bMeOH: solvent; ^cUDP-X can be UDP-galactose or UDP-glucose (Marks et al., 2016).

Compound	^1H (ppm)	^{13}C (ppm)
Acetate	1.92 (s)	—
Alanine	1.48 (d), 3.74 (q)	18.92, 57.1
ATP	8.24 (s), 8.19 (s)	—
Betaine	3.27 (s)	—
Choline	3.20 (s)	54.13
Citrate	2.71 (d), 2.55 (d)	47.4, 47.2
Cystine	3.17, 3.39 (dd)	48.47
DMSO ₂	3.13 (s)	48.56
Formate	8.46 (s)	—
Fumarate	6.51 (s)	—
Fucose	1.22 (s), 2.14, 5.16 (d)	18.46, 23.2, 74.5
GBH isopropylammonium	1.16, 1.30 (d), 3.10, 3.72 (s)	18.84, 22.69, 48.06, 53.77
α,β -Glucose	5.22 (d), 4.64 (d)	—
Glutamate	2.36, 2.27, 2.04	36.31, 36.21, 29.61
Glutamine	2.45, 2.12	34.41, 29.23
Isoleucine	0.95, 0.98 (d)	—
Lactate	1.32 (d), 4.13 (q)	22.5, 64.23
Leucine	0.94 (d), 1.7 (m)	—
Maleate	6.12 (s)	—
Malonate	3.14 (s)	56.15
Mannitol	3.9–3.6	66.2, 72.22, 73.84
MeOH ^b	3.31	51.14
Methionine	2.14	34
1-Methylhistidine	7.88, 7.08	—
Phenylalanine	7.42 (m), 7.38 (m), 7.32 (d),	—
Shikimate	6.44, 4.38, 3.70, 2.74, 2.18	133.36, 69.6, 35.4
Threonine	1.32 (d), 4.24 (q)	22.5, 69.38
Tyrosine	7.19 (d), 6.89 (d)	—
UDP-X ^c	7.96, 7.88, 5.98 (bd)	—
Valine	1.04 (d), 1.00	—

3.2. Chlorophyll fluorescence

Significant differences among the F_v/F_m were found for samples subjected to different concentration of GBH solution (PERMANOVA: pseudo-F = 332.58, $p < 0.001$). Compared to the controls, the maximum yield of the photosystem II photochemical reactions (F_v/F_m) was already significantly reduced at the lowest concentration used (0.5 mg L^{-1}) (Fig. 2a).

3.3. GBH determination in *F. virsoides* thalli calculated by ^1H NMR

A quantitative determination of the herbicide GBH was measured by ^1H NMR Spectroscopy. GBH concentration was

obtained by the integration of both the NMR signals at 3.72 and 1.30 ppm of $\text{CH}_2\text{-N}$ of glyphosate and the methyl groups $(\text{CH}_3)_2$ of isopropylammonium salt, respectively, using the TSP resonance peak as a qualitative and quantitative standard (as described in the Supplementary Information, Section S5) (Cartigny et al., 2008). Due to the unbiased doublet of $(\text{CH}_3)_2$ methyl group at 1.30 ppm, detection of isopropyl ammonium resulted more straightforward (Cartigny et al., 2008). Nevertheless, quantification based on the partially overlapping signals of glyphosate $\text{CH}_2\text{-N}$ at 3.72 ppm gave comparable results. Null concentration was observed in white analytical tanks (without Roundup® solution), while average values (mean \pm SE, $n = 9$) of 0.019 ± 0.003 , 0.041 ± 0.004 and $0.073 \pm 0.007 \mu\text{g mg}^{-1}$ were measured for *F. virsoides* dry weight

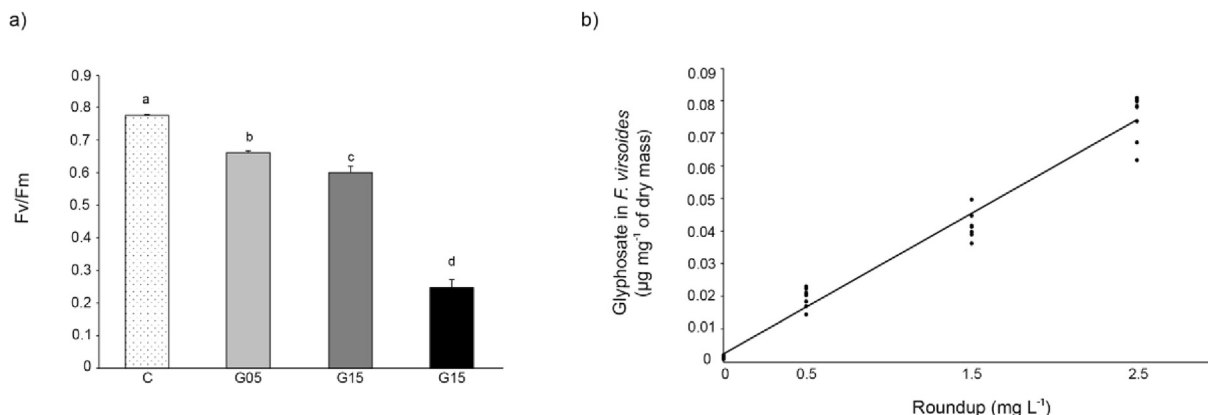


Fig. 2. a) Effects of different treatments on maximum yield of PSII photochemical reactions (F_v/F_m) in *F. virsoides* after 24 h of treatment with Roundup® solution at 0.5 (G05), 1.5 (G15) and 2.5 (G25) mg L^{-1} . Different lower case letters indicate significant differences among treatments ($p < 0.01$). Data are the means \pm SE ($n = 30$). Control (C): sea water. b) Relationships between levels of glyphosate content in dry mass of *F. virsoides* thalli and the different Roundup® concentrations used in the toxicity test.

thalli from tanks enriched with 0.5, 1.5 and 2.5 mg L⁻¹ of Roundup® solution, respectively. This analysis revealed that glyphosate from Roundup® solution accumulated in samples of *F. virsoides* according to a linear relationship (Fig. 2b; $r^2 = 0.9730$, $p < 0.0001$).

3.4. ¹H-NMR-based metabolomics analysis

Multivariate statistical analysis was applied to the whole NMR data of aqueous extracts, focusing on the potential differences in metabolic profiles of *F. virsoides* thalli, collected after a short period of GBH exposure, from tanks enriched with 0.5 mg L⁻¹ (G05), 1.5 mg L⁻¹ (G15) and 2.5 mg L⁻¹ (G25) of Roundup® solution, respectively. The unsupervised analysis (PCA) performed on the whole data revealed a clear group separation, according to a GBH accumulation gradient. In the PCA model (Fig. S2 in SI), the two first principal components (t[1]/t[2]) explained more than 70% of the total variance ($R^2X = 0.71$, $Q^2 = 0.59$). The samples appeared to be partitioned into four clusters corresponding to different levels of GBH exposure (controls, C; 0.5 mg L⁻¹, G05; 1.5 mg L⁻¹, G15 and 2.5 mg L⁻¹, G25), thus indicating that even an unsupervised statistical method can distinguish among the groups of samples and that GBH content appeared as the most significant factor (corresponding NMR signals at 1.14, 1.18, 1.30, 3.72, 3.74, 3.70 ppm). A relatively higher content of polysaccharides moieties was also found in the controls with respect to the herbicide exposed samples (related NMR signals at 3.90, 3.86, 3.82, 3.78, 3.66 ppm). In order to highlight the differences in the samples metabolite content (other than GBH and polysaccharides), the buckets corresponding both to polysaccharides and GBH molecules were excluded from further analyses. The PCA analysis was then repeated and a new PCA model (Fig. S3 in SI) was obtained, with the first two principal components (t[1]/t[2]) explaining about 60% of the total variance ($R^2X = 0.60$, $Q^2 = 0.50$). Moreover, the related PLS-DA (and OPLS-DA) analyses were also obtained to elucidate the most reliable class-discriminating variables that were highly diagnostic for group separation. The PLS-DA model was built using 4 components, obtaining a robust model ($R^2X = 0.73$, $R^2Y = 0.79$, $Q^2 = 0.67$), with Cohen's coefficient (K) equal to 0.9619. The t[1]/t[2] PLS-DA score

plot (Fig. 3a) showed that samples were clustered in distinct groups: in particular, C samples were positioned at positive values of the first axis t[1] (on the right side of the first axis), while thalli exposed to high level of pesticide (G25) were found on the left, at negative values of the first component (t[1]), and resulted the less scattered group. Finally, samples exposed to intermediate levels of GBH groups (G05 and G15, low and intermediate exposure to GBH, respectively) were found between the controls and highly GBH exposed thalli in the t[1]/t[2] PLS-DA score plot. In particular, these samples were mainly distributed at low values of the first component t[1], while resulted well discriminated to each other on the second component t[2], at negative and positive values, respectively. Analogously, the related OPLS-DA model (3 + 1+0 components, $R^2X = 0.73$, $R^2Y = 0.79$, $Q^2 = 0.65$, Fig. 3b) highlighted the different behaviour of G05 samples with respect to G15 and G25 groups, and better describes the progressive sample distribution along the predictive component t[1]. Both PLS-DA and OPLS-DA clearly suggest the specific discriminating metabolite response of algal thalli at low dose with respect to intermediate and high concentration glyphosate exposure. In order to obtain a better discrimination of metabolite levels in groups of samples differently exposed to GBH, supervised pairwise OPLS-DA analyses were performed for GBH exposed samples (G05, G15, G25) with respect to controls (C). In all the three cases (considering the couples C vs G05, C vs G15, C vs G25, Fig. 4a, b, c), the OPLS-DA models were built using one predictive and one orthogonal components, obtaining different model performances, reported in Table 2. The differences in metabolite content were studied by the analysis of the corresponding S-line plot. In all the three cases, controls (C) and GBH exposed samples (G05, G15, G25) were clearly separated on the first predictive component t[1]. This progressive separation (inter-class variability) could be also quantified according to the Q^2 values (reported Table 2) of the obtained OPLS-DA models (Girelli et al., 2016a). The three OPLSDA models (Fig. 4a, b, c) also showed a progressive reduction, according to the increasing GBH exposure, of the variability along the 1st orthogonal component, with respect to the controls. This interesting feature could be related to the smoothing of the natural variability of the metabolic profiles (intra-

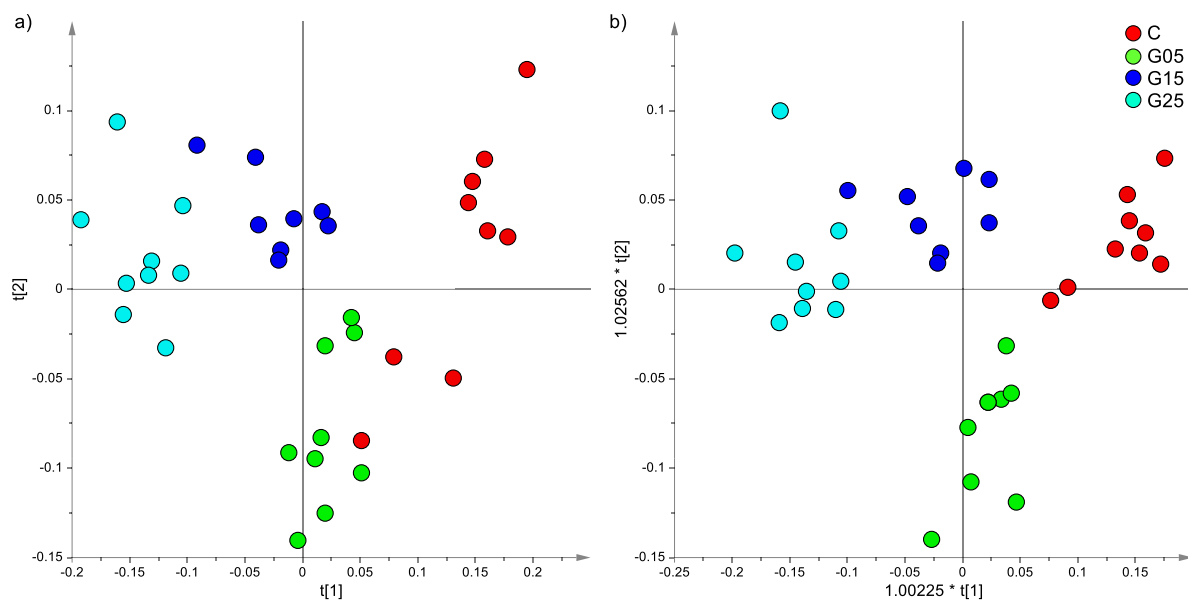


Fig. 3. a) PLS-DA and b) OPLS-DA score plots obtained for aqueous extracts from *F. virsoides* thalli after a short exposure to different Roundup® solutions. C = Controls; G05, G15 and G25 = 0.5, 1.5 and 2.5 mg L⁻¹ of herbicide exposure respectively.

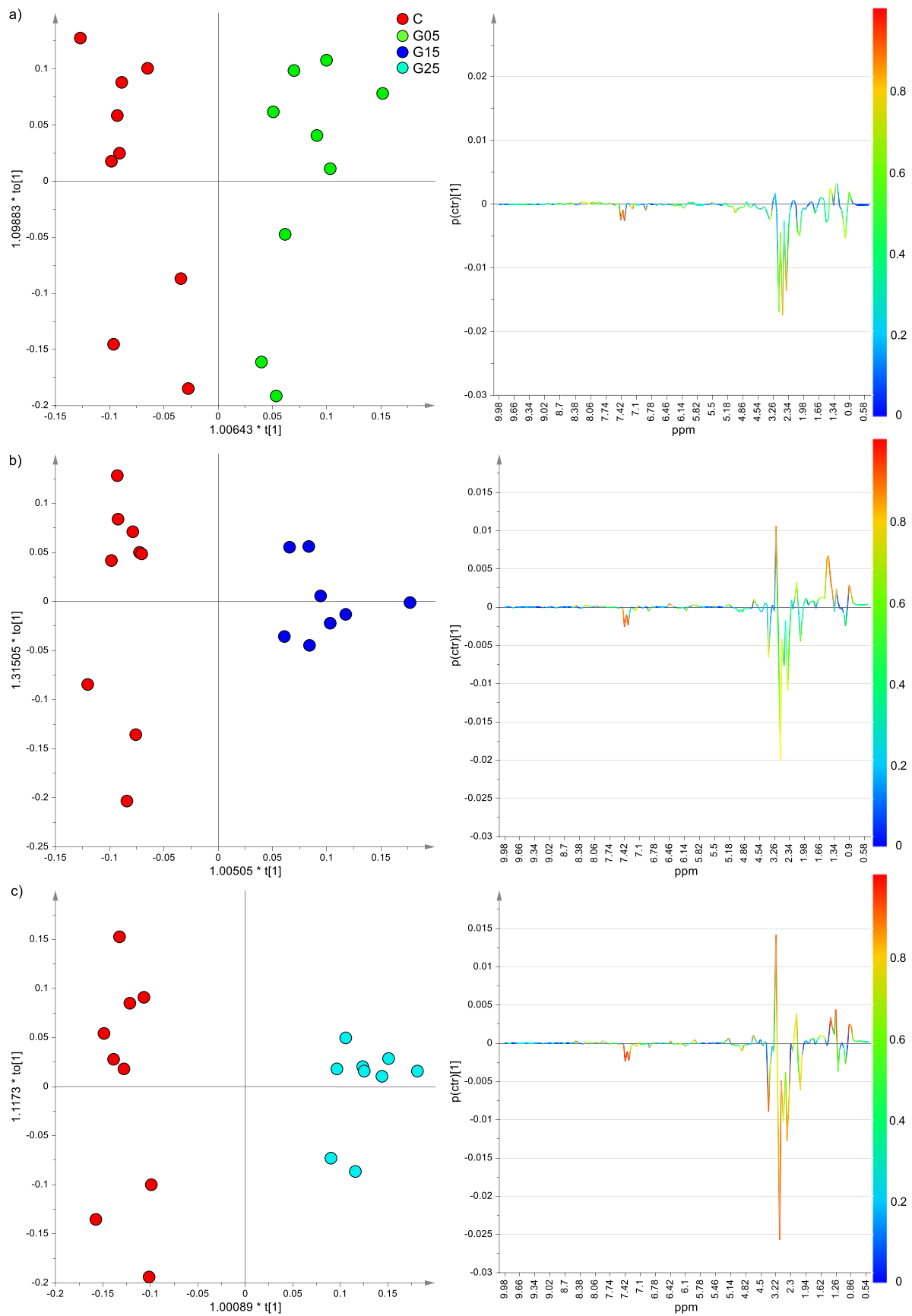


Fig. 4. OPLS-DA score plots (left) and corresponding S-line loading plots (right) regarding pairs comparisons between controls and the different treatments with Roundup® (i.e., a) C vs G05; b) C vs G15; c) C vs G25). Symbols coloured according to the correlation scaled loading $p(\text{corr})$, obtained for aqueous extracts from *F. viscosides* thalli after a short exposure to different treatments. C = Controls; G05, G15 and G25 = 0.5, 1.5 and 2.5 mg L⁻¹ of herbicide exposure respectively.

Table 2

Model performances for the three OPLS-DA score plots reported in Fig. 4. G05, G15, G25 refer to different groups of samples of *F. virsoides* thalli extracts, after 24 h of treatment with Roundup® solution at 0.5, 1.5 and 2.5 mg L⁻¹, respectively. C = controls.

OPLS-DA	model	R ² X	R ² Y	Q ²
C-G05	1 + 1+0	0.66	0.87	0.73
C-G15	1 + 1+0	0.60	0.93	0.84
C-G25	1 + 1+0	0.73	0.97	0.95

class variability) caused by the increasing GBH exposure. By the analysis of the corresponding S-line plots (Fig. 4), the loadings related to the original variables (NMR signals) were obtained allowing to identify the metabolic components distinctive for each group of samples. In general, a decrease in metabolite content was observed in all the samples exposed to the herbicide with respect to controls, together with a relative higher content of shikimate, choline, formate, and glucose. In particular, a significant decrease of glutamate (2.38, 2.34, 2.06 ppm), glutamine (2.46, 2.42, 2.12 ppm), phenylalanine (7.42, 7.38, 7.32 ppm), tyrosine (7.19, 6.89 ppm), isoleucine, leucine (0.98 ppm) and valine (1.04 ppm) and a significant higher relative content of formate (8.46 ppm), mainly characterized G05 samples (exposed to low doses of GBH) with respect to controls (C). A significant decrease in metabolite content, in particular glutamate, phenylalanine, tyrosine and valine and a higher relative content of shikimate (6.44, 2.18 ppm), choline (3.20 ppm), formate (8.46 ppm) and alanine (1.48 ppm) also characterized G15 with respect to controls (C). Finally, a lower content of glutamate, glutamine, malonate, fumarate and a higher content of shikimate, formate, choline and glucose characterized G25 samples with respect to controls (C). Thereafter, relative variation in the metabolite content among groups was also calculated by integration of selected NMR signals using the TSP signal ($\delta = 0.00$ ppm) as internal standard and reported as Log 2 fold change (Supplementary Information, Table S1). One Way-ANOVA with HSD post hoc test for pairwise multiple comparisons of means was performed on the mean integral values of all different groups (Table 3 and Table S2 in Supplementary Information). The complete four classes PLS-DA model of Fig. 3a could also be used as training set to analyze nine samples (labelled as “unknown”, test set) collected in sea waters and potentially exposed to GBH. All the test samples were predicted in the PLS-DA model and resulted into the model space defined by the training set. The prediction analysis classified the test samples mainly between C (controls) and G05 (GBH low level exposure) (Supplementary Information, Fig. S4a). The test set was therefore used for a further focused prediction

analysis, using the specific OPLS-DA model obtained for the two classes (C vs G05, Fig. 4a). In the related predicted scoreplot (Supplementary Information, Fig. S4b), the test samples resulted essentially shifted towards the controls (on the predictive axis), and characterized by an intra-class variability similar to that exhibited by both controls and low GBH exposed samples. The confusion matrix assigned 6 over a total of 9 test samples to C class, while the remaining 3 test samples were included in the G05 group, according to Naïve-Bayes classification (Supplementary Information, Fig. S4b) (Girelli et al., 2016b). Analogously to training set samples, integral values from the NMR spectra were also calculated for the test samples, and significant variation in the metabolite content among groups was evaluated by the ANOVA with HSD post hoc test (Supplementary Information, Table S3). The prediction analysis performed for test samples collected on field and potentially exposed to GBH may suggest the occurrence of the specific contaminant action on the metabolic profiles. Nevertheless, specific residual GBH determination for the on field collected samples and/or appropriate washing out experiments on the model samples should be used to confirm this hypothesis.

4. Discussion

Glyphosate based herbicides (GBHs) are among the most commonly used herbicide worldwide (Annett et al., 2014; Komives & Schröder, 2016). At the beginning of their employment, there was a common consensus that glyphosate was environment-friendly not causing harm to non-target species. Instead, recently, its overuse has been demostred to negatively affect almost all organisms (reviewed by Gill et al., 2018).

In the last years, an increased attention was posed to the potential toxic effects of these substances to non-target organisms and ecosystems. In this study, the presence of glyphosate isopropylamine salt has been clearly identified and quantified in the NMR spectra of aqueous extracts of *F. virsoides*. The high solubility of glyphosate (12,000 mg L⁻¹) facilitates translocation from terrestrial to aquatic environments (Torstensson et al., 2005), where it easily migrates from groundwater to plants. Only few studies have investigated the accumulation of glyphosate in plants, showing a different pattern of uptake among species and between the different parts of a plant (roots vs leaves) (Rzyski et al., 2013; Sikorski et al., 2019). To the best of our knowledge, this is the first study investigating the accumulation of glyphosate in macroalgae. The glyphosate uptake of *F. virsoides* resulted directly proportional to the concentration of chemical in the growth medium, as observed in the common duckweed *Lemna minor* by Sikorski et al. (2019).

Table 3

Metabolite variations (\uparrow : increment, \downarrow : decrement) calculated by the integration of the corresponding selected NMR signals and differences in groups of samples exposed to different concentrations of Roundup® (i.e., G05, G15, G25) with respect to controls (C). Relative statistical significance (Multiple Comparisons of Means, Tukey's honestly significant difference, HSD post hoc test) was set at least at an adjusted p-values <0.05 and indicated with **** 0.001; *** 0.01; ** 0.05; * 0.1.

Metabolite	¹ H NMR chemical shift (ppm)	C vs G05	C vs G15	C vs G25
alanine	1.48	$\uparrow\downarrow$	$\downarrow\uparrow$ ****	$\downarrow\uparrow$
glucose	5.22–4.64	$\downarrow\uparrow$	$\uparrow\downarrow$	$\downarrow\uparrow$ •
choline	3.20	$\downarrow\uparrow$	$\downarrow\uparrow$ ****	$\downarrow\uparrow$ ****
formate	8.46	$\downarrow\uparrow$ •	$\downarrow\uparrow$ ****	$\downarrow\uparrow$ ****
glutamate	2.36	$\uparrow\downarrow$ *	$\uparrow\downarrow$ ****	$\uparrow\downarrow$ ****
glutamine	2.45	$\uparrow\downarrow$ ***	$\uparrow\downarrow$	$\uparrow\downarrow$ ****
isoleucine/leucine	0.98	$\uparrow\downarrow$ ****	$\uparrow\downarrow$	$\uparrow\downarrow$
malonate	3.14	$\uparrow\downarrow$	$\uparrow\downarrow$	$\uparrow\downarrow$ *
fumarate	6.51	$\uparrow\downarrow$	$\uparrow\downarrow$	$\uparrow\downarrow$ *
phenylalanine	7.42	$\uparrow\downarrow$ ****	$\uparrow\downarrow$ ****	$\uparrow\downarrow$ ****
shikimate	6.44	$\downarrow\uparrow$	$\downarrow\uparrow$ ****	$\downarrow\uparrow$ ****
tyrosine	6.89	$\uparrow\downarrow$ ****	$\uparrow\downarrow$ **	$\uparrow\downarrow$ ****
valine	1.04	$\uparrow\downarrow$ ****	$\uparrow\downarrow$ •	$\uparrow\downarrow$

The exposure to different levels of Roundup® produced a general depletion of structural polysaccharides in this brown macroalgae. The effect was already observed at the lowest dose tested in the experiment.

Similarly, the reduction of another integral structural components of the brown algae cell walls, namely phlorotannins, was found in the congeneric *F. vesiculosus* exposed to glyphosate (Pelletreau & Targett, 2008).

Based on this finding, Pelletreau and Targett (2008) suggested that the shikimate pathway, whose presence was experimentally verified only in Rhodophyta and Chlorophyta (Jormalainen & Honkanen, 2008; Bouarab et al., 2004), could be present also in Phaeophyta.

The primary mode of action of glyphosate was, indeed, localized in the shikimate pathway of aromatic amino acid biosynthesis, a pathway that links primary and secondary metabolism. The deregulation of this metabolic pathway affects the synthesis of essential aromatic amino acids and, as a consequence, the synthesis of protein and other secondary metabolites, such as, growth promoters, growth inhibitors, lignin precursors, flavonoids, tannins, and other phenolic compounds (Pérez et al., 2011).

Results of this study seem to confirm the hypothesis of this pathway in brown algae, since a decrease in the aromatic amino acid phenylalanine (PHE) and tyrosine (TYR) content was found in all the samples exposed to Roundup® (at low, intermediate and high levels).

Moreover, as already reported in other studies where a massive accumulation of shikimate was found in cells and tissues of plant exposed to glyphosate (e.g. Bode et al., 1984; Rubin et al., 1984; Gout et al., 1992; Zelaya et al., 2011), we also detect a significant increment of shikimate especially in thalli exposed at intermediate and high doses of Roundup®. This was also found in the non-target aquatic species *Lemna minor* and *Hydrocharis dubia* (Zhong et al., 2018; Sikorski et al., 2019).

A marked effect on amino acid (AA) metabolism, not only the aromatic ones, with a general decrease of the total amount of the dominant AAs, was also found in this study. Specifically, branched-chain AAs (isoleucine, leucine and valine) showed a significant decrease in samples exposed to the lowest concentration of Roundup®, whereas they increase at intermediate and high exposure, suggesting the onset of different responses at different levels of chemical exposure. These findings are consistent with the results of Zou et al. (2014), showing that the branched chain AAs content differently varied in response to acute and chronic stress from copper pollution. A similar pattern was found in a glyphosate-sensitive soybean genotype, in which it was suggested that the deregulation of PHE synthesis caused the increase of alanine and other minor AAs through parallel synthesis pathways (Vivancos et al., 2011). Associated to a decrease in PHE, a reduction of glutamate (GLU) and asparagine and an increase in glutamine and arginine, were found (Vivancos et al., 2011), suggesting that glyphosate is able to trigger the production of AAs with more nitrogen atoms at the expense of their precursors. Probably due to the short time of the experiment, we didn't detect significant differences in the content of nitrogen-rich AAs. However, a significant reduction of GLU was observed in all the thalli exposed to Roundup®.

A moderate increase in glucose content was observed in thalli exposed to high level of Roundup®. Increase in glucose has been associated with a defense response against infection involving shifts in carbohydrate metabolism (Sardans et al., 2014). A significant increase of choline and formate was also observed in the samples exposed to intermediate and high doses of Roundup®, suggesting the onset of stress condition (Sardans et al., 2014).

Among the indirect effects of glyphosate on plant physiology there is, indeed, the onset of oxidative stress (Kremer & Means, 2009; Kielak et al., 2011; Zobiolo et al., 2011; Gomes et al., 2014; Zhong et al., 2018; Sikorski et al., 2019). It is worth noting that this could be another of the secondary effect of the blocked shikimate pathway (Ahsan et al., 2008). Moreover, a prediction analysis on samples collected from sea sites potentially exposed to GBH was also performed. In few cases (3 over 9 test samples), the test samples resulted affected by a metabolomic modification similar to that exhibited by low GBH exposed samples. These results could suggest the hypothesis of low specific contamination occurrence according to their metabolic profiles. Nevertheless, further studies are needed in order to confirm this specific finding.

Finally, even at the lowest Roundup® concentration tested, lower than those tested in previous studies, a significant effect on the photosynthetic activity was found. Values of Fv/Fm in controls were between 0.7 and 0.8, thus indicating an unstressed condition (Maxwell & Johnson, 2000; Ritchie, 2006). In particular, *F. virsoides* was considered to be in a healthy ecophysiological status if the ratio Fv/Fm exceeded 0.70 (Young et al., 2007); a decrease in the value of this variable was considered as a measure of stress (Huppertz et al., 1990; Maxwell & Johnson, 2000), as happened in all treatments with Roundup®. GBHs have been already shown to cause significant changes in chlorophyll content and absorbance and photosynthetic yield in marine macroalgae and seagrasses (Pang et al., 2012; Castro et al., 2015; Kittle & McDermid, 2016; Oliveira et al., 2016; Falace et al., 2018). The mechanisms responsible for the impairment of photosynthetic rate are still not clear. However, some authors suggested that, blocking the shikimate pathway, glyphosate can indirectly inhibit both the biosynthesis of compounds (i.e. quinones, carotenoids and chlorophylls) related to photosynthesis (Dewick, 1998; Fedtke & Duke, 2005) and the Calvin cycle (Gomes et al., 2014), thus irremediately causing the shutdown of photosynthesis.

5. Conclusions

The ecosystem-level effects of glyphosate-based herbicides (GBHs) in coastal waters are still largely unknown. This study showed that native macroalgae in marine habitats may be negatively affected by GBHs. Specifically, we have shown that both productivity and metabolic pathways of aquatic primary producers could show relevant decrease based on the amount of agricultural land use of a certain area. This is of concern since, despite the intense debate on the effects associated with GBH use, these herbicides have not yet been banned or targeted by specific regulation. Available data suggest that the application of glyphosate has grown by 659% in the study area (Friuli Venezia Giulia, NE Italy) over the period 2002 to 2012 (APPA, 2014). In this region, glyphosate is listed as the first priority emerging pollutant, since it exceeds the environmental limits in most of the monitoring sites (ISPRA, 2018; ARPA FVG, 2018).

Macroalgal forests provide critical habitats and food resources to many marine organisms, and are important elements of submarine landscapes. Further investigations on the potential effects of this xenobiotic on marine primary producers should be prioritized, since the adverse effects can be cascaded to higher trophic levels, affecting the functioning of whole ecosystems.

Declarations of interest

None.

Acknowledge

Research funded by the EU Interreg MED AMARE Project (<https://www.msp-platform.eu/projects/amare-actions-marine-protected-areas>).

References

- Ahsan, N., Lee, D.G., Lee, K.W., Alam, I., Lee, S.H., Bahk, J.D., Lee, B.H., 2008. Glyphosate-induced oxidative stress in rice leaves revealed by proteomic approach. *Plant Physiol. Biochem.* 46, 1062–1070. <https://doi.org/10.1016/j.plaphy.2008.07.002>.
- Airolidi, L., Beck, M.W., 2007. Loss, status and trends for coastal marine habitats of Europe. *Oceanogr. Mar. Biol. Annu. Rev.* 45, 345–405. <https://doi.org/10.1201/9781420050943.ch7>.
- Annett, R., Habibi, H.R., Hontela, A., 2014. Impact of glyphosate and glyphosate-based herbicides on the freshwater environment. *J. Appl. Toxicol.* 34, 458–479. <https://doi.org/10.1002/jat.2997>.
- APPA, 2014. Elaborazione dei dati di vendita dei prodotti fitosanitari dal 2002 al 2012 [in Italian]. http://www.appa.provincia.tn.it/fitofarmaci/programmazione_dei_controlli_ambientali/-Criteri_vendita_prodotto_fitosanitari/pagina55.html.
- ARPA FVG, 2018. Rapporto Sullo Stato Dell'ambiente in Friuli Venezia Giulia. http://www.arpa.fvg.it/export/sites/default/istituzionale/consulta/Allegati/RSA_2018/RSA_2018.pdf.
- Arunakumara, K., Walpola, B.C., Yoon, M.H., 2013. Metabolism and degradation of glyphosate in aquatic cyanobacteria: a review. *Afr. J. Microbiol. Res.* 7, 4084–4090. <https://doi.org/10.5897/AJMR12.2302>.
- Barbier, E.B., 2011. Progress and challenges in valuing coastal and marine ecosystem services. *REEP* 6, 1–19. <https://doi.org/10.1093/reep/rer017>.
- Barding, G.A., Béni, S., Fukao, T., Bailey-Serres, J., Larive, C.K., 2012. Comparison of GC-MS and NMR for metabolite profiling of rice subjected to submergence stress. *J. Proteome Res.* 12, 898–909. <https://doi.org/10.1021/pr300953k>.
- Beger, M., Grantham, H.S., Pressey, R.L., Wilson, K.A., Peterson, E.L., Dorfman, D., Mumby, P.J., Lourival, R., Brumbaugh, D.R., Possingham, H.P., 2010. Conservation planning for connectivity across marine, freshwater, and terrestrial realms. *Biol. Conserv.* 143, 565–575. <https://doi.org/10.1016/j.biocon.2009.11.006>.
- Belghit, I., Rasinger, J.D., Heesch, S., Biancarosa, L., Liland, N., Torstensen, B., Waagbø, R., Lock, E.J., Bruckner, C.G., 2017. In-depth metabolic profiling of marine macroalgae confirms strong biochemical differences between brown, red and green algae. *Algal Res* 26, 240–249. <https://doi.org/10.1016/j.algal.2017.08.001>.
- Bilan, M.I., Grachev, A.A., Ustuzhanina, N.E., Shashkov, A.S., Nifantiev, N.E., Usov, A.I., 2002. Structure of a fucoidan from the brown seaweed *Fucus evanescens* C. Ag. *Carbohydr. Res.* 337, 719–730. [https://doi.org/10.1016/S0008-6215\(02\)00053-8](https://doi.org/10.1016/S0008-6215(02)00053-8).
- Bilan, M.I., Shashkov, A.S., Usov, A.I., 2014. Structure of a sulfated xylofucan from the brown alga *Punctaria plantaginea*. *Carbohydr. Res.* 393, 1–8. <https://doi.org/10.1016/j.carres.2014.04.022>.
- Birkemeyer, C., Osmolovskaya, N., Kuchaeva, L., Tarakhovskaya, E., 2018. Distribution of natural ingredients suggests a complex network of metabolic transport between source and sink tissues in the brown alga *Fucus vesiculosus*. *Planta* 249, 377–391. <https://doi.org/10.1007/s00425-018-3009-4>.
- Bode, R., Melo, C., Birnbaum, D., 1984. Mode of action of glyphosate in *Candida maltosa*. *Arch. Microbiol.* 140, 83–85. <https://doi.org/10.1007/BF00409776>.
- Botta, F., Lavison, G., Couturier, C., Alliot, F., Moreau-Guigon, E., Fauchon, N., Guery, B., Chevreuil, M., Blanchoud, H., 2009. Transfer of glyphosate and its degradate AMPA to surface waters through urban sewerage systems. *Chemosphere* 77, 133–139. <https://doi.org/10.1016/j.chemosphere.2009.05.008>.
- Bouarab, K., Adas, F., Gaquerel, E., Kloareg, B., Salaün, J.P., Potin, P., 2004. The innate immunity of a marine red alga involves oxylipins from both the eicosanoid and octadecanoid pathways. *Plant Physiol.* 135, 1838–1848. <https://doi.org/10.1104/pp.103.037622>.
- Burridge, T.R., Gorski, J., 1998. The Use of Biocidal Agents as Potential Control Mechanism for the Exotic Kelp *Undaria Pinnatifida*. Technical Report No. 16. Centre for Research on Introduced Marine Pests, CSIRO Marine Research, Hobart, Australia, ISBN 064306180 0.
- Cartigny, B., Azaroual, N., Imbenotte, M., Mathieu, D., Vermeersch, G., Goullé, J., Lhermitte, M., 2004. Determination of glyphosate in biological fluids by ^1H and ^{31}P NMR spectroscopy. *Forensic Sci. Int.* 143, 141–145. <https://doi.org/10.1016/j.forsciint.2004.03.025>.
- Cartigny, B., Azaroual, N., Imbenotte, M., Mathieu, D., Parmentier, E., Vermeersch, G., Lhermitte, M., 2008. Quantitative determination of glyphosate in human serum by ^1H NMR spectroscopy. *Talanta* 74, 1075–1078. <https://doi.org/10.1016/j.talanta.2007.07.029>.
- Castro, A.J.V., Colares, I.G., Franco, T.C.R., Cultrim, M.V.J., Luvizotto-Santos, R., 2015. Using a toxicity test with *Ruppia maritima* (Linnaeus) to assess the effects of roundup. *Mar. Pollut. Bull.* 91, 506–510. <https://doi.org/10.1016/j.marpolbul.2014.10.006>.
- Catarino, M., Silva, A., Cardoso, S., 2018. Phytochemical constituents and biological activities of *Fucus* spp. *Mar. Drugs* 16, 249. <https://doi.org/10.3390/md16080249>.
- Dewick, P.M., 1998. The biosynthesis of shikimate metabolites. *Nat. Prod. Rep.* 15, 17–58. <https://doi.org/10.1039/NP9951200101>.
- Dunn, W.B., Erban, A., Weber, R., Creek, D., Brown, M., Breiting, R., Hankemeier, T., Goodacre, R., Neumann, S., Kopka, J., Viant, M.R., 2013. Mass appeal: metabolite identification in mass spectrometry-focused untargeted metabolomics. *Metabolomics* 9, 44–66. <https://doi.org/10.1007/s11306-012-0434-4>.
- Eriksson, E., Baun, A., Scholes, L., Ledin, A., Ahlman, S., Revitt, M., Noutsopoulos, C., Mikkelsen, P.S., 2007. Selected stormwater priority pollutants - a European perspective. *Sci. Total Environ.* 383, 41–51. <https://doi.org/10.1016/j.scitotenv.2007.05.028>.
- Fabriceus, K.E., 2005. Effects of terrestrial runoff on the ecology of corals and coral reefs: review and synthesis. *Mar. Pollut. Bull.* 50, 125–146. <https://doi.org/10.1016/j.marpolbul.2004.11.028>.
- Falace, A., Tamburello, L., Guarnieri, G., Kaleb, S., Papa, L., Fraschetti, S., 2018. Effects of a glyphosate-based herbicide on *Fucus virsoides* (Fucales, Ochrophyta) photosynthetic efficiency. *Environ. Pollut.* 243, 912–918. <https://doi.org/10.1016/j.envpol.2018.08.053>.
- Farag, M.A., Porzel, A., Wessjohann, L.A., 2012. Comparative metabolite profiling and fingerprinting of medicinal licorice roots using a multiplex approach of GC-MS, LC-MS and ^1D NMR techniques. *Phytochem* 76, 60–72. <https://doi.org/10.1016/j.phytochem.2011.12.010>.
- Fedtko, C., Duke, S., 2005. In: Hock, B., Elstner, E.F. (Eds.), *Plant Toxicology*. Marcel Dekker, New York, pp. 247–330.
- Gaubert, J., Payri, C.E., Vieira, C., Solanki, H., Thomas, O.P., 2019. High metabolic variation for seaweeds in response to environmental changes: a case study of the brown algae *Lobophora* in coral reefs. *Sci. Rep.* 9, 993. <https://doi.org/10.1038/s41598-018-38177-z>.
- Gill, J.P.K., Sethi, N., Mohan, A., Datta, S., Girdhar, M., 2018. Glyphosate toxicity for animals. *Environ. Chem. Lett.* 16, 401–426. <https://doi.org/10.1007/s10311-017-0689-0>.
- Girelli, C.R., Del Coco, L., Papadia, P., De Pascali, S.A., Fanizzi, F.P., 2016a. Harvest year effects on Apulian EVOOs evaluated by ^1H NMR based metabolomics. *PeerJ* 4, e2740. <https://doi.org/10.7717/peerj.2740>.
- Girelli, C.R., Del Coco, L., Fanizzi, F.P., 2016b. ^1H NMR spectroscopy and multivariate analysis as possible tool to assess cultivars, from specific geographical areas. In: *EVOOs*. Eur J Lipid Sci Techn, 118, pp. 1380–1388. <https://doi.org/10.1002/ejlt.201500401>.
- Girelli, C.R., Del Coco, L., Scorticchini, M., Petriccione, M., Zampella, L., Mastrobuoni, F., Cesari, G., Bertaccini, A., D'Amico, G., Contaldo, N., Migoni, D., Fanizzi, F.P., 2017. *Xylella fastidiosa* and olive quick decline syndrome (CoDiRO) in Salento (southern Italy): a chemometric ^1H NMR-based preliminary study on Ogliarola salentina and Cellina di Nardò cultivars. *Chem Biol Technol Agric* 4, 25. <https://doi.org/10.1186/s40538-017-0107-7>.
- Girelli, C.R., Accogli, R., Del Coco, L., Angilè, F., De Bellis, L., Fanizzi, F.P., 2018. ^1H -NMR-based metabolomic profiles of different sweet melon (*Cucumis melo* L.) Salento varieties: analysis and comparison. *Food Res. Int.* 114, 81–89. <https://doi.org/10.1016/j.foodres.2018.07.045>.
- Gomes, M.P., Smedbol, E., Chalifour, A., Henault-Ethier, L., Labrecque, M., Lepage, L., Lucotte, M., Juneau, P., 2014. Alteration of plant physiology by glyphosate and its by-product aminomethylphosphonic acid (AMPA), an overview. *J. Exp. Bot.* 65, 4691–4703. <https://doi.org/10.1093/jxb/eru269>.
- Gout, E., Bigny, R., Genix, P., Tissut, M., Douce, R., 1992. Effect of glyphosate on plant cell metabolism. ^{31}P and ^{13}C NMR studies. *Biochimie* 74, 875–882. [https://doi.org/10.1016/0300-9084\(92\)90071-L](https://doi.org/10.1016/0300-9084(92)90071-L).
- Greff, S., Zubia, M., Payri, C., Thomas, O.P., Perez, T., 2017a. Chemogeography of the red macroalgae *Asparagopsis*: metabolomics, bioactivity, and relation to invasiveness. *Metabolomics* 13, 33. <https://doi.org/10.1007/s11306-017-1169-z>.
- Greff, S., Aires, T., Serrão, E.A., Engelen, A.H., Thomas, O.P., Pérez, T., 2017b. The interaction between the proliferating macroalga *Asparagopsis taxiformis* and the coral *Astroides calycularis* induces changes in microbiome and metabolomic fingerprints. *Sci. Rep.* 7, 42625. <https://doi.org/10.1038/srep42625>.
- Gügi, B., Le Costaouec, T., Burel, K., P., Helbert, W., Bardor, 2015. Diatom-specific oligosaccharide and polysaccharide structures help to unravel biosynthetic capabilities in diatoms. *Mar. Drugs* 13, 5993–6018. <https://doi.org/10.3390/md13095993>.
- Gupta, V., Thakur, R.S., Reddy, C.R.K., Jhaa, B., 2013. Central metabolic processes of marine macrophytic algae revealed from NMR based metabolome analysis. *RSC Adv.* 3, 7037–7047. <https://doi.org/10.1039/C3RA23017A>.
- Halpern, B.S., Frazier, M., Potapenko, J., Casey, K.S., Koenig, K., Longo, C., Stewart, J.S., Rockwood, R.C., Selig, E.R., Selkoe, K.A., Walbridge, S., 2015. Spatial and temporal changes in cumulative human impacts on the world's ocean. *Nat. Commun.* 6, 7615. <https://doi.org/10.1038/ncomms8615>.
- Hernando, F., Royuela, M., Muñoz-Rueda, A., Gonzalez-Murua, C., 1989. Effect of glyphosate on the greening process and photosynthetic metabolism in *Chlorella pyrenoidosa*. *J. Plant Physiol.* 134, 26–31. [https://doi.org/10.1016/S0176-1617\(89\)80197-X](https://doi.org/10.1016/S0176-1617(89)80197-X).
- Hmelkov, A.B., Zvyagintseva, T.N., Shevchenko, N.M., Rasin, A.B., Ermakova, S.P., 2018. Ultrasound-assisted extraction of polysaccharides from brown alga *Fucus evanescens*. Structure and biological activity of the new fucoidan fractions. *J. Appl. Phycol.* 30, 2039–2046. <https://doi.org/10.1007/s10811-017-1342-9>.
- Huppertz, K., Hanelt, D., Nultsch, W., 1990. Photoinhibition of photosynthesis in the

- marine brown alga *Fucus serratus* as studied in field experiments. Mar. Ecol. Prog. Ser. 66, 175–182. <https://doi.org/10.3354/meps066175>.
- ISPRA, 2018. Rapporto Nazionale Pesticide Nelle Acque - Dati 2015-2016. ISPRA Rapporti, 282/2018. <http://www.isprambiente.gov.it/it/pubblicazioni/rapporti/rapporto-nazionale-pesticidi-nelle-acque-dati-2015-2016-edizione-2018>.
- IUCN, 2016. The IUCN Red List of Threatened Species. Version 2015-4. <http://www.iucnredlist.org>.
- Jégou, C., Kervarec, N., Cérantola, S., Bihannic, I., Stiger-Pouvreau, V., 2015. NMR use to quantify phlorotannins: the case of *Cystoseira tamariscifolia*, a phloroglucinol-producing brown macroalga in Brittany (France). Talanta 135, 1–6. <https://doi.org/10.1016/j.talanta.2014.11.059>.
- Jormalainen, V., Honkanen, T., 2008. Macroalgal chemical defenses and their roles in structuring temperate marine communities. In: Amsler, C.D. (Ed.), Algal Chemical Ecology. Springer, Berlin, Heidelberg, pp. 57–89. https://doi.org/10.1007/978-3-540-74181-7_3.
- Kielak, E., Sempruch, C., Mioduszewska, H., Klocek, J., Leszczyński, B., 2011. Phytotoxicity of Roundup Ultra 360 SL in aquatic ecosystems: biochemical evaluation with duckweed (*Lemna minor* L.) as a model plant. Pestic. Biochem. Physiol. 99, 237–243. <https://doi.org/10.1016/j.pestbp.2011.01.002>.
- Kittle, R.P., McDermid, K.J., 2016. Glyphosate herbicide toxicity to native Hawaiian macroalgal and seagrass species. J. Appl. Phycol. 28, 2597–2604. <https://doi.org/10.1007/s10811-016-0790-y>.
- Komives, T., Schröder, P., 2016. On glyphosates. Ecocycles 2, 1–8. <https://doi.org/10.19040/ecocycles.v2i2.60>.
- Kremer, R.J., Means, N.E., 2009. Glyphosate and glyphosate-resistant crop interactions with rhizosphere microorganisms. Eur. J. Agron. 31, 153–161. <https://doi.org/10.1016/j.eja.2009.06.004>.
- Kreutzweiser, D., Kingsbury, P., Feng, J., 1989. Drift response of stream invertebrates to aerial applications of glyphosate. Bull. Environ. Contam. Toxicol. 42, 331–338. <https://doi.org/10.1007/BF01699957>.
- Li, B., Lu, F., Wei, X., Zhao, R., 2008. Fucoidan: structure and bioactivity. Molecules 13, 1671–1695. <https://doi.org/10.3390/molecules13081671>.
- Liu, X., Yang, C., Zhang, L., Li, L., Liu, S., Yu, J., You, L., Zhou, D., Xia, C., Zhao, J., Wu, H., 2011. Metabolic profiling of cadmium-induced effects in one pioneer intertidal halophyte *Suaeda salsa* by NMR-based metabolomics. Ecotoxicology 20, 1422–1432. <https://doi.org/10.1007/s10646-011-0699-9>.
- Lotze, H.-K., Lenihan, H.S., Bourque, B.J., Bradbury, R.H., Cooke, R.G., Kay, M.C., Kidwell, S.M., Kirby, M.X., Peterson, C.H., Jackson, J.B.C., 2006. Depletion, degradation, and recovery potential of estuaries and coastal seas. Science 312, 1806–1809. <https://doi.org/10.1126/science.1128035>.
- Marks, V., Munoz, A., Rai, P., Walls, J.D., 2016. ¹H NMR studies distinguish the water soluble metabolomic profiles of untransformed and RAS-transformed cells. PeerJ 4, e2104. <https://doi.org/10.7717/peerj.2104>.
- Maxwell, K., Johnson, G.N., 2000. Chlorophyll fluorescence - a practical guide. J. Exp. Bot. 51, 659–668. <https://doi.org/10.1093/jexbot/51.345.659>.
- Mercurio, P., Flores, F., Mueller, J.F., Carter, S., Negri, A.P., 2014. Glyphosate persistence in seawater. Mar. Pollut. Bull. 85, 385–390. <https://doi.org/10.1016/j.marpolbul.2014.01.021>.
- Mitchell, D.G., Chapman, P.M., Long, T.J., 1987. Acute toxicity of Roundup and Rodeo herbicides to rainbow trout, chinook, and coho salmon. Bull. Environ. Contam. Toxicol. 39, 1028–1035. <https://doi.org/10.1007/bf01689594>.
- Nödler, K., Licha, T., Voutsas, D., 2013. Twenty years later – atrazine concentrations in selected coastal waters of the Mediterranean and the Baltic Sea. Mar. Pollut. Bull. 70, 112–118. <https://doi.org/10.1016/j.marpolbul.2013.02.018>.
- Nylund, G.M., Weinberger, F., Rempt, M., Pohnert, G., 2011. Metabolomic assessment of induced and activated chemical defence in the invasive red alga *Gracilaria vermiculophylla*. PLoS One 6, e29359. <https://doi.org/10.1371/journal.pone.0029359>.
- Oliveira, R.D., Boas, L.K., Branco, C.C., 2016. Assessment of the potential toxicity of glyphosate-based herbicides on the photosynthesis of *Nitella microcarpa* var. *wrightii* (Charophyceae). Phycologia 55, 577–584. <https://doi.org/10.2216/16-12.1>.
- Orlando-Bonaca, M., Mannoni, P.A., Poloniato, D., Falace, A., 2013. Assessment of *Fucus viriosides* distribution in the Gulf of Trieste (Adriatic Sea) and its relation to environmental variables. Bot. Mar. 56, 451–459. <https://doi.org/10.1515/bot-2013-0027>.
- Palanisamy, S.K., Arumugam, V., Rajendran, S., Ramadoss, A., Nachimuthu, S., Magesh, P.D., Sundaresan, U., 2018. Chemical diversity and anti-proliferative activity of marine algae. Nat. Prod. Res. 25, 1–5. <https://doi.org/10.1080/14786419.2018.1488701>.
- Pang, T., Liu, J., Liu, Q., Zhang, L., Lin, W., 2012. Impacts of glyphosate on photosynthetic behaviours in *Kappaphycus alvarezii* and *Neosiphona savatieri* detected by JIP-test. J. Appl. Phycol. 24, 467–473. <https://doi.org/10.1007/s10811-012-9796-2>.
- Pelletreau, K.N., Targett, N.M., 2008. New perspectives for addressing patterns of secondary metabolites in marine macroalgae. In: Amsler CD Editor. Algal Chemical Ecology. Springer Berlin Heidelberg, pp. 121–146. https://doi.org/10.1007/978-3-540-74181-7_6.
- Pérez, G.L., Solange Vera, M., Miranda, L.A., 2011. Effects of herbicide glyphosate and glyphosate-based formulations on aquatic ecosystems. In: Kortekamp, A. (Ed.), Herbicides and Environment. InTech, Argentina, pp. 343–368. <https://doi.org/10.5772/12877>.
- Relyea, R.A., 2005. The lethal impact of Roundup on aquatic and terrestrial amphibians. Ecol. Appl. 15, 1118–1124. <https://doi.org/10.1890/04-1291>.
- Ritchie, R.J., 2006. Consistent sets of spectrophotometric chlorophyll equations for acetone, methanol and ethanol solvents. Photosynth. Res. 89, 27–41. <https://doi.org/10.1007/s11210-006-9065-9>.
- Rizzo, C., Genovese, G., Morabito, M., Faggio, C., Pagano, M., Spanò, A., Zammuto, V., Minicante, S.A., Manghisi, A., Cigala, R.M., 2017. Potential antibacterial activity of marine macroalgae against pathogens relevant for aquaculture and human health. JPAM 11, 1695–1706. <https://doi.org/10.22207/JPAM.11.4.07>.
- Rubin, J.L., Gaines, C.G., Jensen, R.A., 1984. Glyphosate inhibition of 5-enolpyruvylshikimate 3-phosphate synthase from suspension-cultured cells of *Nicotiana glauca*. Plant Physiol. 75, 839–845. <https://doi.org/10.1104/pp.75.3.839>.
- Rzymycki, P., Klimaszuk, P., Kubacki, T., Poniedziałek, B., 2013. The effect of glyphosate based herbicide on aquatic organisms – a case study. Limnol. Rev. 4, 215–220. <https://doi.org/10.2478/limre-2013-0024>.
- Sáenz, M., Di Marzio, W., Alberdi, J., del Carmen Tortorelli, M., 1997. Effects of technical grade and a commercial formulation of glyphosate on algal population growth. Bull. Environ. Contam. Toxicol. 59, 638–644. <https://doi.org/10.1007/s001289900527>.
- Salem, F.B., Essid, N., Boufahja, F., Louati, H., Beyrem, H., Mahmoudi, E., 2016. Impacts of glyphosate on a free-living marine nematode community: results from microcosm experiments. J. Coast Zone Manag 19, 434. <https://doi.org/10.4172/2473-3350.1000434>.
- Sardans, J., Gargallo-Garriga, A., Pérez-Trujillo, M., Parella, T., Seco, R., Filella, I., Penuelas, J., 2014. Metabolic responses of *Quercus ilex* seedlings to wounding analysed with nuclear magnetic resonance profiling. Plant Biol. 16, 395–403. <https://doi.org/10.1111/plb.12032>.
- Schaffer, J., Sebetch, M., 2004. Effects of aquatic herbicides on primary productivity of phytoplankton in the laboratory. Bull. Environ. Contam. Toxicol. 72, 1032–1037. <https://doi.org/10.1007/s00128-004-0347-7>.
- Sikorski, L., Baciak, M., Beś, A., Adomas, B., 2019. The effects of glyphosate-based herbicide formulations on *Lemna minor*, a non-target species. Aquat. Toxicol. 209, 70–80. <https://doi.org/10.1016/j.aquatox.2019.01.021>.
- Sobolev, A.P., Brosio, E., Gianferri, R., Segre, A.L., 2005. Metabolic profile of lettuce leaves by high-field NMR spectra. Magn. Reson. Chem. 43, 625–638. <https://doi.org/10.1002/mrc.1618>.
- Stachowski-Haberhorn, S., Becker, B., Marie, D., Haberhorn, H., Coroller, L., Broise, D., 2008. Impact of Roundup on the marine microbial community, as shown by an in situ microcosm experiment. Aquat. Toxicol. 89, 232–241. <https://doi.org/10.1016/j.aquatox.2008.07.004>.
- Thibaut, T., Pinedo, S., Torras, X., Ballesteros, E., 2005. Long-term decline of the populations of Fucales (*cystoseira* spp. and *sargassum* spp.) in the alberes coast (France, north-western mediterranean). Mar. Pollut. Bull. 50, 1472–1489. <https://doi.org/10.1016/j.marpolbul.2005.06.014>.
- Torstenson, L., Börjesson, E., Stenström, J., 2005. Efficacy and fate of glyphosate on Swedish railway embankments. Pest Manag. Sci 61, 881–886. <https://doi.org/10.1002/ps.1106>.
- Vendrell, E., Ferraz, D.G., Sabater, C., Carrasco, J.M., 2009. Effect of glyphosate on growth of four freshwater species of phytoplankton: a microplate bioassay. Bull. Environ. Contam. Toxicol. 82, 538–542. <https://doi.org/10.1007/s00128-009-9674-z>.
- Vivanco, P.D., Driscoll, S.P., Bulman, C.A., Ying, L., Emami, K., Treumann, A., Mauve, C., Noctor, G., Foyer, C.H., 2011. Perturbations of amino acid metabolism associated with glyphosate-dependent inhibition of shikimic acid metabolism affect cellular redox homeostasis and alter the abundance of proteins involved in photosynthesis and photorespiration. Plant Physiol. 111–181024. <https://doi.org/10.1104/pp.111.181024>, 2011.
- Wang, C., Lin, X., Li, L., Lin, S., 2016. Differential growth responses of marine phytoplankton to herbicide glyphosate. PLoS One 11, e0151633. <https://doi.org/10.1371/journal.pone.0151633>.
- Ward, J.L., Harris, C., Lewis, J., Beale, M.H., 2003. Assessment of ¹H NMR spectroscopy and multivariate analysis as a technique for metabolite fingerprinting of *Arabidopsis thaliana*. Phytochemistry 62, 949–957. [https://doi.org/10.1016/S0031-9422\(02\)00705-7](https://doi.org/10.1016/S0031-9422(02)00705-7).
- Waycott, M., Duarte, C.M., Carruthers, T.J.B., Orth, R.J., Dennison, W.C., Olyarnik, S., Calladine, A., Fourqurean, J.W., Heck Jr., K.L., Hughes, A.R., Kendrick, G.A., Kenworthy, W.J., Short, F.T., Williams, S.L., 2009. Accelerating loss of seagrasses across the globe threatens coastal ecosystems. Proc. Natl. Acad. Sci. 106, 12377–12381. <https://doi.org/10.1073/pnas.0905620106>.
- Widenfalk, A., Bertilsson, S., Sundh, I., Goedkoop, W., 2008. Effects of pesticides on community composition and activity of sediment microbes e responses at various levels of microbial community organization. Environ. Pollut. 152, 576–584. <https://doi.org/10.1016/j.envpol.2007.07.003>.
- Wu, H., Wang, W.X., 2011. Tissue-specific toxicological effects of cadmium in green mussel (*Perna viridis*): nuclear magnetic resonance-based metabolomics study. Environ. Toxicol. Chem. 30, 806–812. <https://doi.org/10.1002/etc.446>.
- Wu, H., Liu, X., Zhao, J., Yu, J., 2011. NMR-based metabolomic investigations on the differential responses in adductor muscles from two pedigrees of Manila clam *Ruditapes philippinarum* to cadmium and zinc. Mar. Drugs 9, 1566–1579. <https://doi.org/10.3390/md9091566>.
- Wu, H., Liu, X., Zhao, J., Yu, J., 2012. Toxicological responses in halophyte *Suaeda salsa* to mercury under environmentally relevant salinity. Ecotoxicol. Environ. Saf. 85, 64–71. <https://doi.org/10.1016/j.ecoenv.2012.03.016>.
- Young, E.B., Dring, M.J., Savidge, G., Birkett, D.A., Berges, J.A., 2007. Seasonal variations in nitrate reductase activity and internal N pools in intertidal brown algae are correlated with ambient nitrate concentrations. Plant Cell Environ. 30, 764–774. <https://doi.org/10.1111/j.1365-3040.2007.01666.x>.
- Zelaya, I.A., Anderson, J.A., Owen, M.D., Landes, R.D., 2011. Evaluation of

- spectrophotometric and HPLC methods for shikimic acid determination in plants: models in glyphosate-resistant and-susceptible crops. *J. Agric. Food Chem.* 1 59, 2202–2212. <https://doi.org/10.1021/jf1043426>.
- Zhang, L., Liu, X., You, L., Zhou, D., Wu, H., Zhao, J., Feng, J., Yu, J., 2011. Metabolic responses in gills of Manila clam *Ruditapes philippinarum* exposed to copper using NMR-based metabolomics. *Mar. Environ. Res.* 72, 33–39. <https://doi.org/10.1016/j.marenvres.2011.04.002>.
- Zhong, G., Zhonghua, W., Liu, N., Yin, J., 2018. Phosphate alleviation of glyphosate-induced toxicity in *Hydrocharis dubia* (Bl.) Backer. *Aquat. Toxicol.* 91–98. <https://doi.org/10.1016/j.aquatox.2018.05.025>, 2011.
- Zobiolo, L.H.S., Kremer, R.J., Oliveira, R.S., Constantim, J., 2011. Glyphosate affects chlorophyll, nodulation and nutrient accumulation of “second generation” glyphosate-resistant soybean (*Glycine max* L.). *Pestic. Biochem. Physiol.* 99, 53–60. <https://doi.org/10.1016/j.pestbp.2010.10.005>.
- Zou, H.X., Pang, Q.Y., Lin, L.D., Zhang, A.Q., Li, N., Lin, Y.Q., Li, L.M., Wu, Q.Q., Yan, X.F., 2014. Behavior of the edible seaweed *Sargassum fusiforme* to copper pollution: short-term acclimation and long-term adaptation. *PLoS One* 9, e101960. <https://doi.org/10.1371/journal.pone.0101960>.